# Experimental study of the 4*d* ionization continuum in atomic iodine by photoelectron and photoion spectroscopy

Laurent Nahon,* Agneta Svensson,† and Paul Morin†
*Laboratoire pour l'Utilisation du Rayonnement Electromagnétique, Bâtiment 209d, Université Paris–Sud, 91405 Orsay CEDEX, France*
(Received 8 October 1990)

Iodine atoms, produced by laser-induced dissociation of molecular iodine, have been photoionized with synchrotron radiation in the region of the $4d \rightarrow \epsilon f$ shape resonance. By using photoelectron spectroscopy in conjunction with ionic spectroscopy, we have measured the 4*d*, 5*p*, 5*s*, and valence satellites' absolute photoionization cross sections, as well as the relative oscillator strengths for the production of $I^+$, $I^{2+}$, and $I^{3+}$. Some specific open-shell effects have been observed such as the strong 4*d*-5*p* hole electrostatic coupling, as revealed by the 4*d* photoelectron spectrum, and the weak enhancement of the outer-shell cross sections, especially the 5*p* one, in the region of the $4d \rightarrow \epsilon f$ shape resonance, as compared with xenon. Multiple-electron processes associated with 4*d* photoemission have been studied and account for about 20% of the photoabsorption cross section. Moreover, as already pointed out in iodine compounds, the total oscillator strength of atomic iodine is found, in the studied spectral region, to be surprisingly weak.

## I. INTRODUCTION

Since the late 1960s, a lot of work has been devoted by both experimentalists and theoreticians to the study of photoionization of closed-shell systems, since they are easy to produce in the form of monoatomic vapors, and since their spherical symmetry simplifies the theoretical calculations. Among them, rare gases, and especially xenon ($Z=54$) have become a showcase for atomic inner-shell photoionization[1] for which the agreement between theory and experiment is now very good. Both experimentalists[2–6] and theoreticians[7–10] have pointed out the importance of multielectron processes, relaxation effects, and intershell coupling in the description of the 4*d*, 5*s*, and 5*p* subshell photoionization of xenon for which a $4d \rightarrow \epsilon f$ giant shape resonance has been observed for the first time by Ederer in 1964.[11] This resonance, interpreted by Wendin[7] in terms of a collective response to the electromagnetic field, originates in a one-electron picture, from the diffusion of the outgoing photoelectron by the centrifugal barrier of the effective 4*d* potential.[12]

In contrast with the abundant literature concerning closed-shell systems, very little work has been done, up to now, on the photoionization of open-shell systems, especially atomic halogens. With the exception of the total-ion-yield measurements of Samson, Shefer, and Angel on chlorine[13] and the absorption work of Pettini, Mazzoni, and Tozzi on iodine,[14] their experimental studies have been limited to He I photoelectron spectroscopy[15–17] (PES), and to photoionization studies of atomic iodine at 80 eV, which has pointed out both experimentally and theoretically the strong electrostatic coupling between the 4*d* and the 5*d* hole as revealed on the PES of the 4*d* subshell.[18] In addition, the decay of the $4d \rightarrow 5p$ excitation at 46.2 eV has been studied in a recent work.[19] Despite its evident theoretical interest, we find the same situation concerning theoretical calculations. For atomic iodine ($Z=53$), to which attention is now addressed, except for the work of Manson *et al.*[20] concerning the 5*p* outer-shell photoionization, the only theoretical work on the 4*d* continuum has been done by Combet-Farnoux and Ben Amar[21] in an *LS* coupling scheme using the coupled-channels method[8] and has emphasized the importance of coupling all the channels opened by the multiplet structure; the 4*d* cross section was found to be very close to the one of xenon. However, atomiclike $4d \rightarrow \epsilon f$ shape resonances have been observed in numerous iodine compounds such as $CH_3I$ (Refs. 22-24), $I_2$ (Ref. 25), HI (Ref. 26), and $C_2F_4IBr$ (Ref. 27) for which, when absolute cross sections are available, the 4*d* cross section is found to be surprisingly much less intense than in the case of xenon.

In this paper, we wish to report on the 4*d* photoionization of atomic iodine, observed for the first time by use of synchrotron radiation (SR), in the 60–130-eV photon-energy range and to compare it with previous studies of xenon and $I^-$ (Ref. 28) on the one hand, and of iodine compounds, on the other hand, in order to stress the influence of the open 5*p* outer shell on the photoionization of a shallow inner shell such as the 4*d* one. With this aim, we have used both PES and photoion spectroscopy that are very useful and complementary techniques. Indeed, PES provides partial cross sections of the 4*d*, 5*s*, and 5*p* subshells allowing the study of intershell coupling between them, whereas photoion spectroscopy accounts for the absorption spectrum and allows us to distinguish between various decay processes associated with the 4*d* hole. Moreover, with our technique, we are able to provide absolute photoionization cross sections by simple branching-ratio measurements (see Sec. II), thus spectra discussed in Sec. III, will be presented on absolute scales. A description of the experimental procedure is presented in Sec. II. Brief concluding remarks are given in Sec. IV.

 

## II. EXPERIMENT

The experimental procedure, namely the production of atomic iodine by laser photodissociation of $I_2$, has already been used in a first work[18] and improved in a recent one.[19] The experimental setup is described in detail elsewhere[29] and will be presented here briefly except for some slight modifications. From an oven heated to about 100 °C, we evaporate solid iodine to obtain through a very thin nozzle (0.3 mm diam) a narrow effusive jet of gas which crosses a focused laser beam at right angle originating from an argon-ion laser used in a multiline mode (mostly 514 and 488 nm). This laser beam photodissociates, *in situ,* the molecular iodine, inducing mainly a transition to the $(^1\Pi_{1u})$ repulsive state[30] to produce iodine atoms in the $(^2P_{3/2})$ ground state.

The synchrotron radiation emitted from the Super Anneau de Collisions d'Orsay (Super ACO) storage ring and monochromatized by a 2.5 m toroidal grating monochromator, crosses the interaction zone where it photoionizes the iodine atoms. In the new geometry used for the present work, the two photon beams are collinear, and no longer perpendicular, which will allow us in the near future to measure the angular distribution of the photoelectrons since the 127° cylindrical analyzer is able to rotate with respect to the photon beams. For this study, electrons and ions have been detected at the magic angle of 54.7° with respect to the polarization vector of the incident vuv photon, in order to cancel, according to Yang's formulas, angular effects in the particles' ejection.[31] Thus, spectra recorded at this angle yield branding-ratio data directly and relative cross sections after correction for the transmission of the analyzer and for photon-flux variations that were monitored by a molybdenum mesh.

Performing several PES at 21.21 eV, with different laser power, we have shown[29] that we are able, with a laser power of about 8 W in the chamber, to induce a quasicomplete photodissociation; typically, more than 95% of the signal originates from the atoms. We have thus realized a very pure and stable source of atomic iodine, much more efficient than the one used in a previous work,[18] and adapted to PES.

To achieve photoion spectroscopy, we have used our electron analyzer but with inverse polarities. An electric plate with a hole, located 10 mm before the exit of the nozzle was set at a positive potential $V$ to extract the ions into the analyzer. For total-ion-yield spectroscopy, $V$ was a constant potential, whereas for time-of-flight (TOF) spectroscopy, $V$ was pulsed with a 100-$\mu$s period. The time difference between the pulse and the arrival of an ion onto the channeltron was recorded in a multichannel analyzer through a time-to-amplitude converter. The resolution achieved with a 5 $V$ per cm electric field, is quite poor as compared to the conventional TOF technique using a drift tube, but was good enough to easily resolve the $I^{3+}$, $I^{2+}$, and $I^+$ expected peaks. The accuracy of such a simple system is about 10% for the photon-energy-dependence yield of a given ion. The change from the electron to the ion mode was done in a few minutes without opening the chamber. We were thus able to check the dissociation yield during the TOF operation, by looking at the PES of the 5$p$ or 4$d$ subshells.

One of the main advantages of this radical production method is that absolute photoionization cross sections can be derived from simple branching ratios, according to the following formula, valid at the magic angle:

$$n\frac{S_{\text{fragment}}}{\sigma_{\text{fragment}}}=\frac{\Delta S_{\text{parent}}}{\sigma_{\text{parent}}},$$

where in the case of iodine $n$ is a stochiometric coefficient equal to 0.5. $S_{\text{fragment}}$ represents the atomic iodine signal, while $\Delta S_{\text{parent}}$ is the decrease of the molecular iodine signal after the laser has been turned on and $\sigma$ is the absolute photoionization cross section of a given subshell of the molecule or the atom. The knowledge of $\sigma_{\text{parent}}$ leads to the determination of $\sigma_{\text{fragment}}$. This normalization procedure has been checked at 21.21 eV photon energy, where we have measured the ratio of the relative cross section of the 5$p$ subshell of atomic iodine to the one of the $5p\sigma$ and $5p\pi$ subshells of molecular iodine and compare it with the same ratio derived by De Lange, Vander-Meulen, and Van der Meer in the case of bromine[17] for the 4$p$, $4p\sigma$, and $4p\pi$ subshells (direct checking of our normalization procedure was not possible owing to the lack of absolute measurements for atomic iodine). These ratios should be nearly equal since, at 21.21 eV photon energy, the 4$p$ subshell of atomic bromine and the 5$p$ subshell of atomic iodine exhibit the same behavior;[20] the $Z$-dependent effects are compensated since we compare ratios. Indeed, we measured a ratio of 0.30 in the case of iodine which is in very good agreement with the value of 0.31 measured in bromine. In Sec. III, we will use the absolute photoabsorption cross section of $I_2$ which has been measured by Comes, Nielsen, and Schwarz[25] in the 50–150-eV energy range, to provide absolute scales to the different presented spectra, according to the present normalization procedure.

## III. RESULTS AND DISCUSSION

In Sec. III A, we will focus on the partial cross sections of the 4$d$, 5$s$, and 5$p$ subshells of atomic iodine, which will be discussed and compared to similar results in iodine compounds and xenon. Then, in Sec. III B, the different ionic contributions extracted from TOF spectra will be presented, and results concerning multielectron excitations will be derived, in order to provide an absolute cross-section scale to the absorption spectrum presented and discussed in Se. III C in terms of oscillator strength.

### A. Partial cross sections

#### *1. 4d subshell*

In Fig. 1, we present two PES, recorded with a SR photon energy of 80 eV; they are corrected only for a flat background of about 10% of the maximum intensity and for the transmission of the analyzer. The monochromator was operated with ~0.2-eV energy-band pass and the energy pass of the analyzer was 5 eV, providing a resolu-

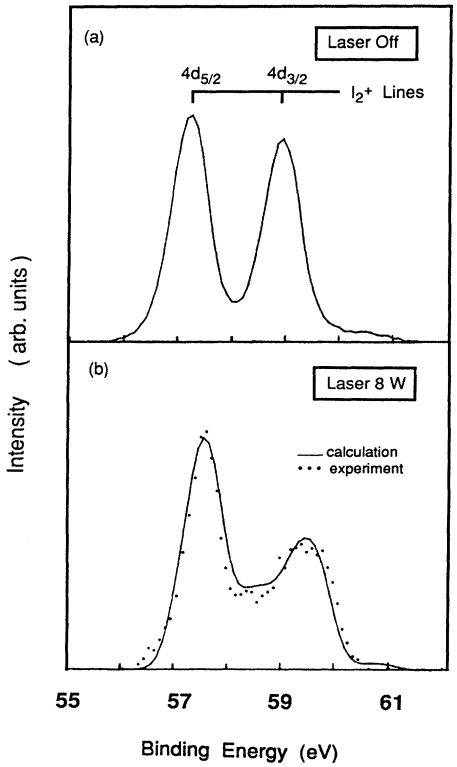


FIG. 1. 4*d* inner-shell PES, recorded at 80 eV photon energy; (a) laser off and (b) laser at 8 W, with the theoretical calculation curve from Ref. 18 given by a solid line. The overall resolution is 0.42 eV.

tion of 0.37 eV; the overall resolution was ~0.42 eV. The spectrum of Fig. 1(a) was recorded laser "off," showing the $4d_{5/2}$ and $4d_{3/2}$ lines of molecular iodine in very good agreement with previous work.[32] These lines can be labelled with an atomic notation since the coupling with the molecular field can be neglected, as demonstrated by the resemblance of this PES with the 4*d* subshell in xenon. The spectrum of Fig. 1(b) has been obtained with a laser power of 8 W in the chamber. The dissociation is nearly complete since the molecular peak at 57.15 eV is not detectable; the dissociation rate was also checked looking at the $5p^{-1}$ atomic lines at lower photon energy which are more characteristic.[29] This spectrum shows the $I(4d^{-1})$ states presenting a complex multiplet structure due to the strong coupling of the 5*p* and 4*d* holes in the $4d^9 5s^2 5p^5$ ionic configuration. Solid line represents the 12 lines calculated by Combet-Farnoux,[18] convoluted with our experimental resolution. The agreement is very good; comparison with the same spectrum obtained in a previous work[18] shows a significant improvement due to the absence of secondary electrons, which were generated by the optical fiber used to carry the laser beam into the chamber. This calculation has been done in an intermediate coupling scheme, necessary to give account for the broad multiplet structure of this open-shell system, due to the strong electrostatic interaction. The various lines, distributed in a nonstatistical ratio, are extended over 2.5 eV instead of 1.76 eV as calculated in a *LS* coupling scheme,[33] 1.7 eV in $I_2$ and 1.97 eV in xenon.[34]

According to the formula given in Sec. II, one can derive the ratio between the absolute photoionization cross section of molecular and atomic iodine by measuring the area of the two spectra presented in Fig. 1. At 80 eV, one finds $\sigma(I)/\sigma(I_2)=0.30$. Note that this value is less than the one we obtain in the simplest picture where $\sigma(I)$ is half of $\sigma(I_2)$. Let us now derive an absolute cross section for the 4*d* subshell of atomic iodine at 80 eV which will be our normalization reference for the photon-energy-dependent spectra presented further. This photon energy has been chosen as a good compromise between the increase in the photoionization cross section with increasing photon energy and the decrease in the analyzer transmission with increasing electron energy. By recording PES at 80 eV of the "4*d*" subshell and satellites as well as outer subshells of molecular iodine, we estimate the contribution of the "4*d*" subshell to the absorption to be 80%±5%. Comes, Nielsen, and Schwarz[25] have measured a value of 19 Mb for the absorption cross section of $I_2$ at 80 eV. We thus obtain a value of 4.6 Mb for the 4*d* subshell photoionization cross section of atomic iodine at 80 eV photon energy.

In Fig. 2 are shown cross-section results, obtained by recording PES at various photon energies, for the sum of the 12 multiplet components of the 4*d* subshell in atomic iodine, which have been scaled according to the normalization procedure explained above; spectra have been corrected for photon-flux variations and for the analyzer transmission. By analogy to the case of xenon, for which the 4*f* orbital has a strong continuum character so that excitation to this virtual orbital contributes significantly to the photoionization process, the observed resonance in atomic iodine can be identified as a shape resonance due to the strong centrifugal barrier in the $4d^9\epsilon f$ outgoing channel, responsible for the delayed onset and for the increase of the cross section to 90 eV. At still higher ener-

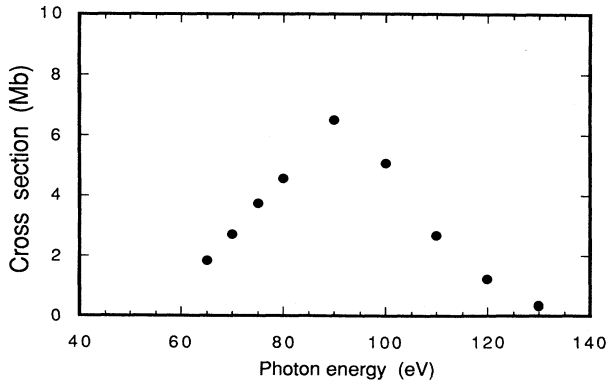


FIG. 2. Partial cross section for the sum of the 12 components of the I 4*d* subshell multiplet scaled at 80 eV to the photoabsorption measurement of Comes, Nielsen, and Schwarz (Ref. 25) concerning $I_2$. The photon resolution is a constant 0.7 Å full width at half maximum. Errors bars are approximately 10%, except for the first and the two last points (~15%).

gy, the $4d \rightarrow \epsilon f$ dipole matrix element experiences a change in sign and causes a Cooper minimum. The general trends of these shape resonances can be described, in a one-electron picture, as follows: As we go from Cs ($Z=55$) to Xe ($Z=54$), I ($Z=53$), and Te ($Z=52$) the centrifugal barrier increases while the electrostatic potential decreases, the necessary kinetic energy at the cross-section maximum (which is the pertinent parameter) thus grows by a few eV for each step,[35] while the trapping of the photoelectron is becoming weaker, the lifetime of the quasibound state is decreasing which causes a broadening in the cross-section spectrum, and its maximum is decreasing by about 15% for each $Z$, from a wave-function overlap argument.[36] Nevertheless, many-body effects have to be included for a correct description of the 4*d* shape resonance, especially to give account for its width.[7] These resonances are not expected to be very sensitive to the chemical environment nor the phase (gas or solid) of the studied species, since they are very localized on the absorbing atoms.[12] Thus, results concerning atomic iodine should not be very far from those observed in iodine compounds. The situation concerning the 4*d* subshell photoionization shape resonances for xenon (the case of tellurium will be presented in Sec. III C, concerning the absorption spectrum, because no partial 4*d* cross sections are available to the knowledge of the authors) as well as for several iodine compounds is resumed in Table I.

The position of the 4*d* resonance in atomic iodine is in good agreement with the general trends given above, as well as its width, which is perhaps a little bit underestimated by our measurements. The very suspicious values published by Pettini, Mazzoni, and Tozzi[14] must be due to a saturation effect in their absorption measurements, as revealed by the non-Lorentzian shape of the $4d \rightarrow 5p$ resonance they observe. But the most striking feature concerns the measured maximum intensity of the resonance, which is for $I_2$, $CH_3I$, and especially for I, much weaker than the one expected as compared with Xe. Even if the possible errors concerning the results of Comes, Nielsen, and Schwarz[25] in $I_2$ are such that a 50% higher value for the maximum intensity is possible, it gives an upper limit of about 15 Mb per atom in $I_2$ and 10 Mb in I, in good agreement with the case of $CH_3I$, which is still surprising as compared with Xe. In Sec III B, we will focus on the relative strength of multielectron processes in order to see if they can account for the missing oscillator strength of the 4*d* subshell in the 60–130-eV photon-energy range, as compared with xenon.

On the contrary to the case of a closed-shell system such as Xe for which the agreement between theory and experiment is now excellent, the theory is not able, up to now, to account for this unexpected feature observed in atomic iodine. The unique calculation about the 4*d* photoionization cross section in atomic iodine[21] has been done in *LS* coupling, which is not the appropriate coupling scheme as discussed earlier. The discrepancy between the 4*d* calculated thresholds in *LS* coupling (energy spread of 1.7 eV) and in intermediate coupling (energy spread of 2.5 eV) points out the limitations of these calculations, as revealed by the calculated position of the maximum which is 10 eV higher than the one observed in atomic iodine and iodine compounds. Moreover, it does not take into account intershell coupling, or relaxation effects which can reduce the maximum intensity of the 4*d* subshell by 30% in Xe (Ref. 37) and nearly 40% in the case of Ba.[38] Photoabsorption calculations on $I^-$ (Ref. 28) do not take into account relaxation effects, or any open-shell effects, as an evidence.

Up to now, we have considered the 4*d* cross section for the sum of the unresolved 12 multiplet components. We wish to focus, now, on the variations of the branching ratios between these components, as a function of photon energy. As our resolution does not allow the separation

TABLE I. Shape resonance parameters of the 4*d* subshell photoionization cross section in I, $I^-$, Xe, and several iodine compounds.

| | I expt.[a] | I expt.[b] | I theor.[c] | $I^-$ theor.[d] | $CH_3I$[e] | $I_2$[f] | HI[h] | Xe expt.[i] | Xe theor.[j] |
|---|---|---|---|---|---|---|---|---|---|
| Position of the maximum (eV) | 91 | 74 | 100 | 94 | 88 | 90 | 92 | 100 | 100 |
| Kinetic energy at the maximum (eV) | 34 | 17 | 43 | 37 | 30 | 33 | 34 | 32 | 32 |
| Width at half maximum (eV) | 38 | 19 | 47 | 41 | 42 | 42 | 41 | 39 | 41 |
| Maximum intensity (Mb) | 6.5 | | 30 | 27 | 11 | 10[g] | | 22 | 22 |

[a]Present work.
[b]Absorption measurements from Ref. 14.
[c]From Ref. 21.
[d]From Ref. 28.
[e]From Ref. 24.
[f]4*d* photoionization contribution from Ref. 25.
[g]Per atom.
[h]From Ref. 26.
[i]From Ref. 5.
[j]From Ref. 10.

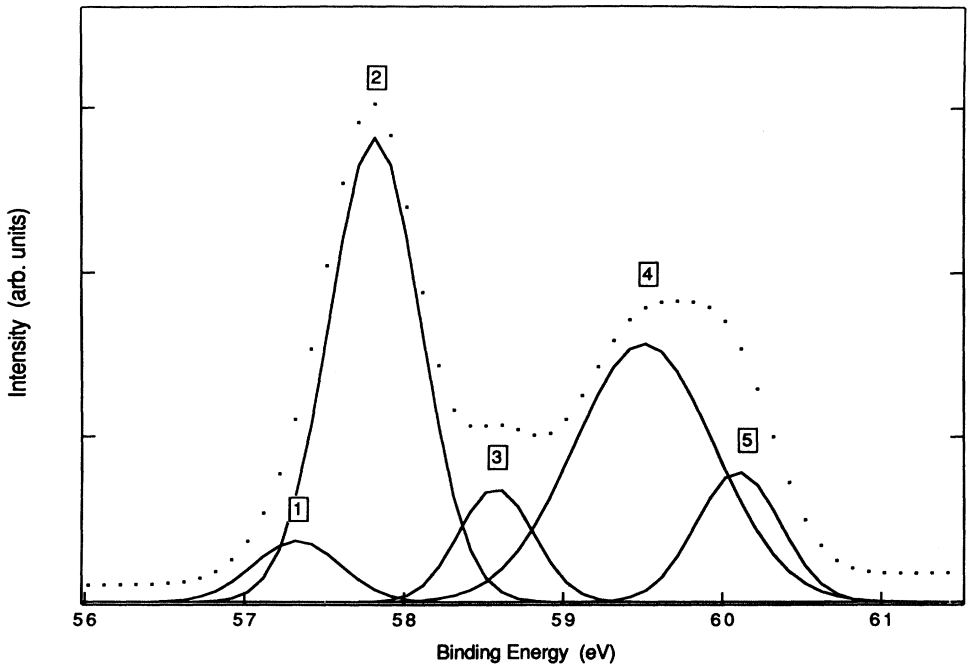


FIG. 3. PES of atomic iodine recorded at 100 eV, with an overall resolution of 0.45 eV, displayed here by dots. Solid lines represent the decomposition of this spectrum into five major bands, labeled 1 to 5.

of each of the 12 components, we have decomposed the various 4*d* subshell PES in five major bands as shown in Fig. 3. We have derived the branching-ratio dependence upon the photon energy of these five bands, as plotted in Fig. 4. The general trend is the following: After a disturbed situation close to the threshold, the different branching ratios become nearly constant (within the error bars) from 75 to 120 eV, converging to a value close to

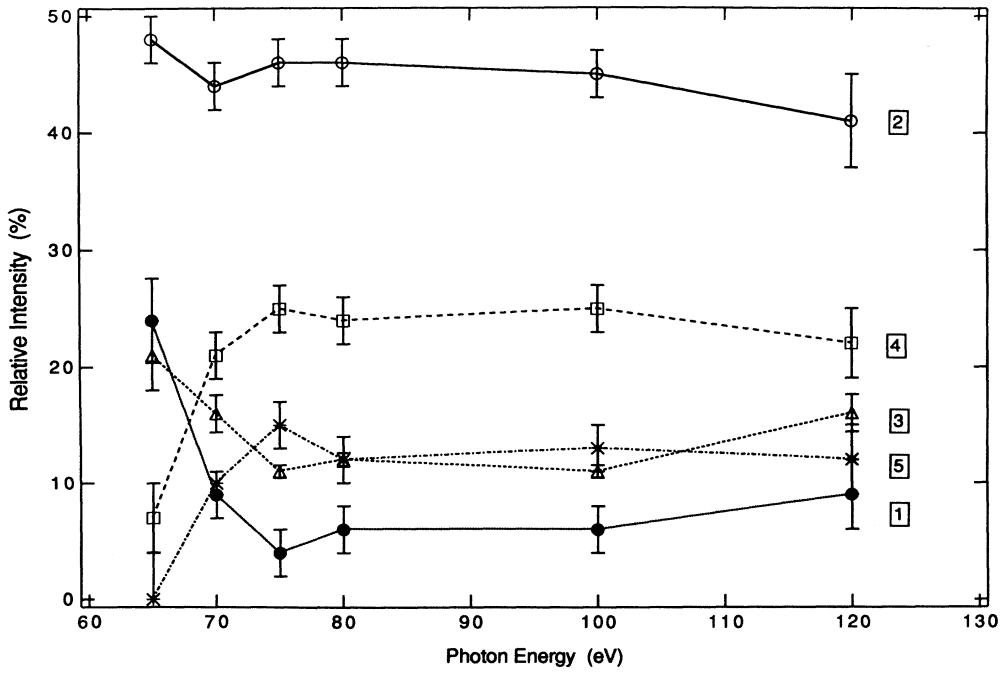


FIG. 4. Evolution of the branching ratios of the five peaks defined in Fig. 3, with photon energy. Errors bars are linked to the accuracy of the decomposition and to the counting rates of the recorded PES.

one deduced from calculations.[18] The reason why these calculations, including only geometrical effects, account so well for the PES recorded at 80 eV (see Fig. 1), is that at this photon energy it seems that there are no more dynamical effects. This kind of behavior has already been observed in xenon[39,40] and in $CH_3I$ (Ref. 24) and can be partially explained by a kinetic-energy effect. In the near-threshold photon-energy range, peaks labelled 1, 2, and 3 have a higher kinetic energy than peaks 4 and 5, and thus are further along in their sharp increase in the cross section due to the shape resonance (see Fig. 2).

We thus conclude that the open-shell effect is mostly a static effect, namely geometric, as revealed by the broad multiplet structure of the PES presented in Fig. 1(b) (very different from the PES of closed-shell species such as $I_2$ and Xe), and not a dynamic one, except at low kinetic energies. However, the accuracy of our data, is not, actually, sufficient to bring a precise quantitative description of these dynamical effects; the present work should be completed by a study of asymmetry parameters which could bring information about phase shifts between the 12 multiplet components..

### 2. 5p and 5s subshells

In Fig. 5, are shown results concerning the photoionization of the outer shells in atomic iodine, namely the 5p, 5s subshells and valence satellites, scaled to the 4d cross section. These satellite states, whose binding energies are spread over ~6 eV between 23.5 and 29.3 eV, are due to the strong configuration interaction between the $5s^15p^5(^1P)$ configuration and mostly the $5s^25p^3(^2P)5d(^1P)$ and $5s^25p^3(^2D)5d(^1P)$ ones, and to 5p shake-up excitations converging to the double-ionization limit, as demonstrated in a previous work.[19] It is interesting to note that the behavior of the satellites is similar in both iodine and xenon, in which the $5s^15p^6(^2S)$ configuration is mostly mixed with the $5s^25p^45d$, $5s^25p^46d$, and $5s^25p^46s$ ones.[4] Indeed, at 65 eV, we measure a satellite to 5s cross-section ratio of 0.5 to be compared to the value of 0.74 in xenon at 68.9 eV and 0.72 at 74.8 eV,[4] while in the energy range of the "5s Cooper minimum,"[41] this ratio is of about 3 in iodine at 45 eV (Ref. 19) and 7 in xenon at 35 eV. We thus confirm the importance of electron correlations in the region where the 5s cross section is small.

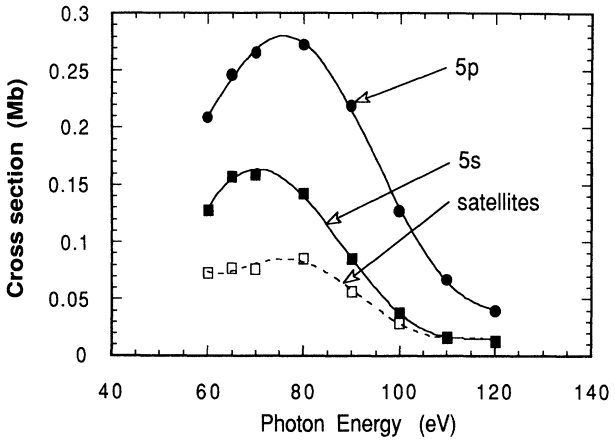


FIG. 5. Partial cross sections of the 5p, 5s subshells and valence satellites, scaled to the absolute 4d cross section of Fig. 2. Satellites are due to configuration interaction, mostly with the $5s^25p^3(^2P)5d$ and $5s^25p^3(^2D)5d$ configurations, and 5p shake-up excitations. Their lines are spread over ~6 eV between 23.5 and 29.3 eV binding energy (see Ref. 19). Errors bars are approximately 10%, except for the two last points of the 5p curve (~15%) and the three last points of 5s and satellite curves (~20%). Lines given are simple polynomial fits as a guide to the eye.

The most striking feature of the curves presented in Fig. 5 is the enhancement of the outer-shell cross sections in the energy region of the maximum of the 4d shape resonance, due to the intershell coupling which transfers part of the 4d oscillator strength onto the outer shells. At still higher energy, the 5p and 5s subshells decrease affected by the 4d Cooper minimum. This behavior, already observed in xenon,[2,5,6] Ba, and lanthanides,[42] is the signature of electron correlations among the 4d, 5s, and 5p subshells. As in Ba and Xe the outer-shell cross sections peak at photon energies about 15 eV below the energy of the maximum of the 4d cross section. However, in the case of iodine, the enhancement of the outer-shell cross sections (as measured between the 4d threshold and the photon energy of the maximum for the outer-shell cross sections) is +35%, which is much weaker than the value of +150% measured in the case of xenon.[2] The 5p+5s+satellite cross section is ~0.52 Mb at the maximum which represents about 9% of the 4d cross section, whereas in Xe this value is 2.4 Mb which represents 16% of the 4d cross section.[5] A possible explanation could be that these outer shells have given part of their oscillator strength in the region of the strong resonance $4d \rightarrow 5p$ which mostly decays through direct autoionization into the outer-shell channels.[19] This is not the case with the $4d \rightarrow 6p$ resonances in Xe, for which autoionization into the outer-shell channels amounts to less than 0.5% of the total decay rate.[43] Another explanation emerges from the weakness of the absolute 4d cross section in iodine which could reduce the strength of the inter-shell coupling, as compared with xenon.[44] The weakness of the enhancement is more pronounced for the 5p subshell, of which the cross section represents at its maximum (~75 eV) only 5% of the 4d cross section, whereas the 5s cross section represents about 2.8% of the 4d one. In Xe, at its maximum (~85 eV), this value is 10% for 5p and 3.2% for 5s.[5] Thus, the presence of the hole in the 5p subshell of iodine seems to reduce the strength of the intershell coupling between the 5p and 4d subshells, whereas the coupling between the 5s and the 4d subshells is close to the one existing in Xe; this gives evidence of an open-shell effect. However, the coupling between the 4d and the 5p subshells is still important enough to modify the photoionization cross section of the 5p subshell, as revealed by the very strong discrepancy between our results and the 5p cross section calculated by Manson *et al.*[20] without any intershell coupling, while the same calculations in atomic chlorine reproduce quite well the general behavior of the experimental photoionization cross section measured by Samson, Shefer, and Angel.[13]

### B. Ion spectroscopy and 4*d* many-electron processes

Ionization of an inner-shell electron leads to a temporary highly excited state of the ion, which in turn relaxes to a lower energy state. PES brings partial cross sections directly attributed to the production of one given excited state as soon as one electron is involved, which is not the case of one-step double ionization. On the other hand, ion spectroscopy gives information about the different decay of all populated channels, such as Auger decay and associated shake processes involving the ejection and/or excitation of many electrons simultaneously or sequentially. Partitioning of all those processes has been the matter of numerous studies concerning xenon,[5,6,40,45] in which the measured intensity of the 4*d* multielectron processes was found higher than 20% of the 4*d* cross section in the region of the shape resonance maximum.

In order to study multielectron processes and to investigate if they can account for the missing oscillator strength that we measure for the 4*d* partial cross section in atomic iodine, as compared to Xe, we have performed TOF spectra at several photon energies. The area of a given TOF line is related to the cross section for the production of an ion of a given charge. All the spectra have been corrected for photon-flux variations, and we have checked that the sum of the three ionic contributions was equal to the total-ion yield we measured separately. The relative partial cross sections for the production of the singly, doubly, and triply charged ions are plotted in Fig. 6. As in Xe,[6] the singly charged ion yield peaks at about 15 eV below ($\sim$75 eV) the maximum of the 4*d* shape resonance, which mimics the behavior of the outer-shell cross sections (see Fig. 5), whereas the triply charged ion curve peaks at about 5 eV above the $4d \rightarrow \epsilon f$ cross-section maximum ($\sim$95 eV). Moreover, as in Xe, Cs, Ba (Ref. 46), and La (Ref. 47), the total-ion yield is dominated by the doubly and triply charged ion yields, mostly due to Auger decay processes, showing the strong continuum character of the 4*f* orbital in this region of the periodic table; it is not the case in Dy (Ref. 47), Sm, and Eu (Ref. 46), where the strong autoionization in the $4f^{-1}$ channel following the $4d \rightarrow 4f$ excitation induces domination of the singly charged ion yield over a multicharged ion yield.

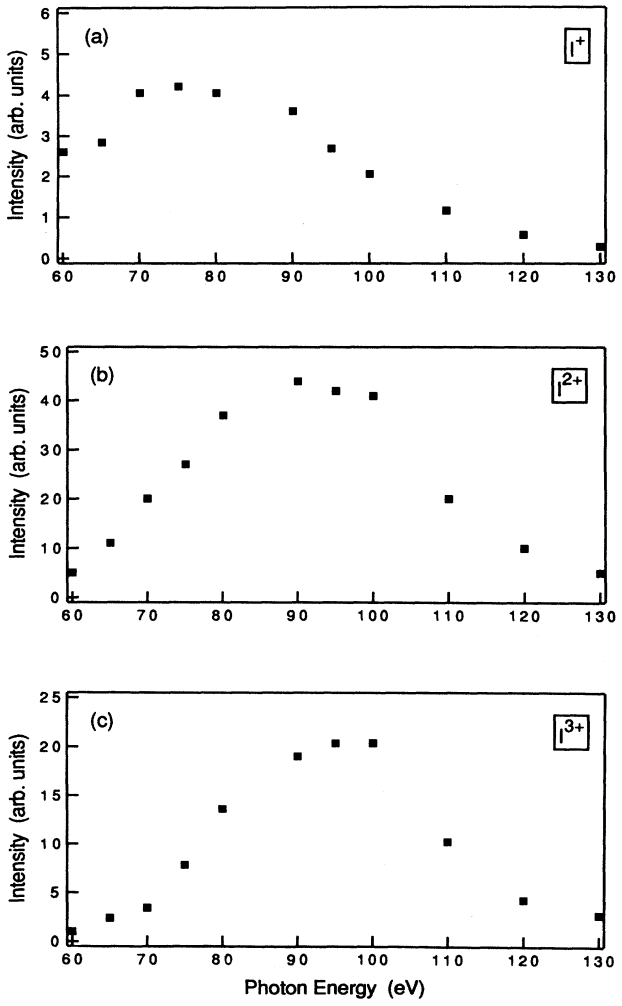


FIG. 6. Relative oscillator strength for the production of (a) $I^+$, (b) $I^{2+}$, and (c) $I^{3+}$. Error bars are approximately 10%, except for the first and the two last points of each curve ($\sim$20%).

In order to get an estimation of the importance of multielectron processes in the case of iodine, we have to connect the photoionization cross sections, presented in Sec. III A, to the present charge-resolved ion yields. [The accuracy of our data does not allow a precise determination owing to false coincidences due to ions created during the extraction period, which induces some uncertainty in the normalization of the curve presented in Fig. 6(c).] Neglecting postcollision interaction, fluorescence decay (justified for the 4*d* shell of a midheavy atom), and direct triple ionization, ion-yield cross sections can be decomposed into the various contributing photoionization cross sections as follows:[5]

$$N\mathcal{I}(I^+) = \sigma_{5sp^+} + \sigma_{(5sp^+)^*} , \tag{1}$$

$$N\mathcal{I}(I^{2+}) = \sigma_{5sp^{2+}} + \sigma_{4d^+}(1-\alpha) + \sigma_{(4d^+)^*}(1-\alpha') , \tag{2}$$

$$N\mathcal{I}(I^{3+}) = \alpha\sigma_{4d^+} + \alpha'\sigma_{(4d^+)^*} + \sigma_{4d^{2+}} , \tag{3}$$

where $\sigma_{5sp^+}$ represents the sum of 5*p* and 5*s* cross section, $\sigma_{(5sp^+)^*}$ the valence ionization plus excitation cross section (satellite bands in Fig. 5), $\sigma_{5sp^{2+}}$ the valence direct double ionization (shake-off) cross section. A similar notation is used for the 4*d* subshell: $\sigma_{4d^+}$ represents the cross section for the creation of a 4*d* hole followed by a simple $(1-\alpha)$ or double and cascade $(\alpha)$ Auger process, $\sigma_{(4d^+)^*}$ represents the cross section for the creation of a 4*d* hole with simultaneous excitation of a valence electron followed by a single $(1-\alpha')$ or double and cascade $(\alpha')$ Auger process, and $\sigma_{4d^{2+}}$ represents the cross section for the creation of a 4*d* hole with simultaneous ionization of a valence electron followed by a simple Auger process. $N$ is a normalization constant and $\mathcal{I}$ is the reported intensities in Fig. 6.

By measuring the ion-yield ratio $\sigma(I^+)/\sigma(I^{2+})$ at 45 eV photon energy (using an aluminum filter to get rid of

second-order light), where 4d channels are not yet opened, we have estimated the valence shake-off fraction, supposed constant in the 45–130-eV photon-energy range, as 45(±5)% of the total valence, single photoionization cross section, close to the xenon value of 46%.[40] From our ion-yield values at 65 eV photon energy, where multielectron processes involving a 4d electron are not yet allowed energetically, we have derived the normal Auger rate $1-\alpha=0.80$ (±0.04) to be compared with the 0.76 value in the case of Xe.[5] From Eq. (1), we extract a mean value of $N=0.12$ (±0.005), which gives a total-ion-yield cross section of 7.8 Mb at 90 eV. Resolving Eqs. (1), (2), and (3), and from the knowledge of the total valence photoionization cross section as $1.45(\sigma_{5sp^+}+\sigma_{(5sp^+)^*})$ and assuming $\alpha$ and $\alpha'$ constant, we derive the "4d shake" cross section, namely the sum of the cross section of the multielectron processes involving a 4d electron $\sigma_{(4d^+)^*}+\sigma_{4d^{2+}}$. Results are plotted in Fig. 7. The shake contribution is about 20%±10%. This strong error bar explains the slightly negative cross section found for the two first points of the shake cross section. Nevertheless, we have an estimation of the behavior of the 4d shake processes, which is found comparable to the case of xenon, and thus these multielectron processes cannot account for a high part of the missing oscillator strength when we compare atomic iodine and xenon.

### C. Absorption spectrum and total oscillator strength

Now that we have studied all the different processes which can contribute to photoabsorption, we present, in Fig. 8, a total-ion-yield spectrum in the 60–130-eV photon-energy range, which is, as we neglect the fluorescence decay, equivalent to an absorption spectrum. It has been corrected for photon-flux variation and normalized to an intensity of about 7.8 Mb at 90 eV photon energy according to the sum of ionic contributions presented below. The total error bar in the normalization is about 25%. The agreement with the "sum" curve in Fig. 7 is satisfactory, in view of the error bars which explain the slight difference concerning the width, mostly due to an underestimation of the 4d shake processes contribution in the low-photon-energy part of the spectrum.

As in the case of other atoms located in the same region of the periodic table, the absorption spectrum is dominated by the $4d\rightarrow\epsilon f$ shape resonance and thus mimics the behavior of the 4d partial cross-section spectrum of Fig. 2. So the shape, width, and position of this gross feature in the absorption spectrum of iodine follow the general trends, as was the case for the 4d partial cross section. Moreover, as in Xe,[48] a shoulder is observed at about 13–18 eV above the first 4d threshold (70–75 eV), which we assign to $4d^{-1}5p^{-1}$nl shake-up processes.[45]

We now resume the situation concerning the intensity of the absorption spectrum in the 4d shape resonance photon-energy region, and discuss it in terms of oscillator strength. To get a more quantitative understanding of the absorption spectrum presented in Fig. 8, we have calculated $N_{\text{eff}}$, the effective number of electrons, whose oscillator strength is exhausted within the energy range covered by our measurements:

$$N_{\text{eff}}=113\int_{60}^{130}\sigma_a(\lambda)/\lambda^2 d\lambda\ ,$$

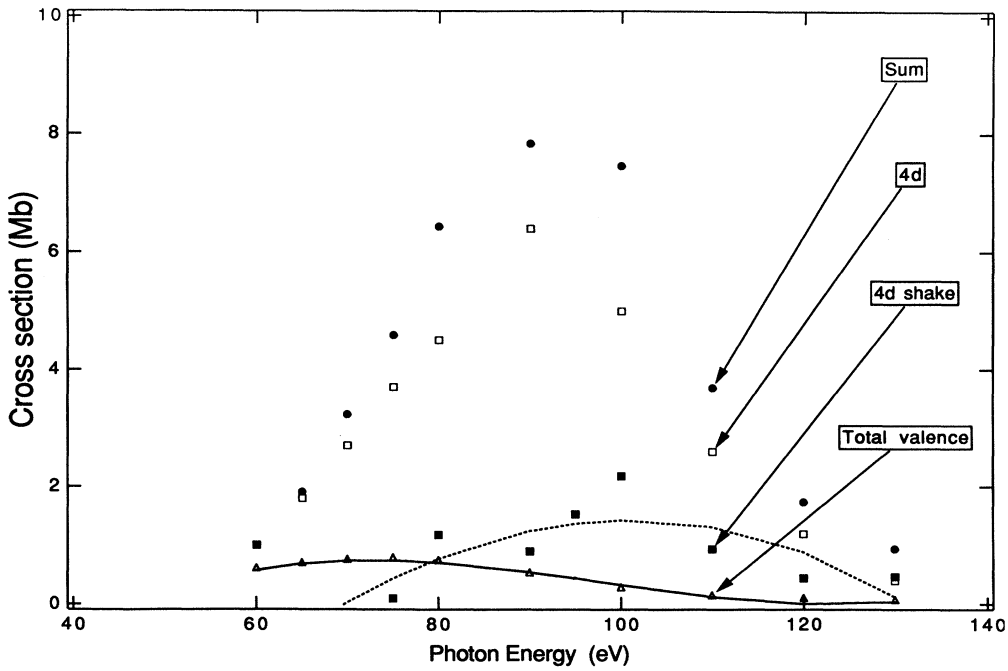


FIG. 7. Absolute cross sections for the 4d direct photoionization, 4d shake processes (shake-up and shake-off), total valence photoionization (including shake-up and shake-off transitions), and the sum of all photoionization processes, as derived from the procedure presented in Sec. III B. Solid (dashed) line is a simple polynomial fit given here as a guide to the eye concerning the total valence (4d shake processes) contribution.

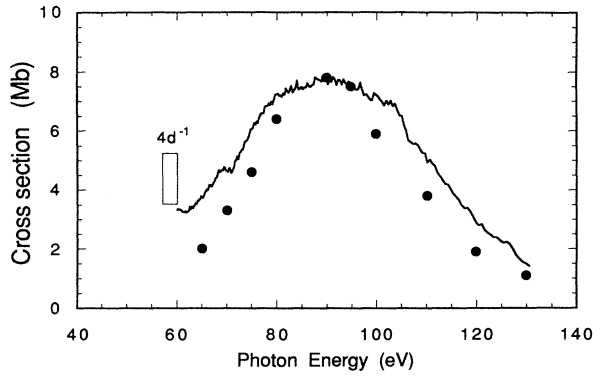


FIG. 8. Continuous total-ion-yield spectrum, scaled at 90 eV photon energy on the "sum" curve of Fig. 7, displayed are by dots. The photon resolution is a constant 0.4 Å half width at half maximum. The rectangle represents the energy spread of the 12 $4d^{-1}$ thresholds.

where $\sigma_a(\lambda)$ is the total photoabsorption cross section at wavelength $\lambda$. We obtain a value of about 3.2 electrons to which one has to add 0.3 due to the $4d \rightarrow 5p$ discrete excitations.[49] We thus obtain a total value for $N_{\text{eff}}$ of about 3.5 electrons for all the processes involving the excitation or/and ionization of a $4d$ electron to 130 eV. This value is lower than the five effective electrons per atom derived by Comes, Nielsen, and Schwarz[25] in $I_2$, which is related to the already unexpected value of 0.30 for the $\sigma_{4d}(I)/\sigma_{4d}(I_2)$ ratio at 80 eV. The $N_{\text{eff}}$ value for $I_2$ is already small as compared to the case of Xe, in solid and gas phases as well as in the fluorinated compounds $XeF_2$ and $XeF_4$,[50] for which $N_{\text{eff}} \sim 11$ within the first-continuum hump,[48] whereas the second low and broad maximum contributes about 3, to $N_{\text{eff}}$. These numbers add up to about 14 for the total $N_{\text{eff}}4d$ transition which is the predicted value for the $4d \rightarrow \epsilon f$ transitions in the one-electron approximation.[51] ($4d \rightarrow \epsilon p$ transitions do not contribute significantly to the $4d$ ionization continuum.[52]) Our $N_{\text{eff}}$ value is still low if we look at the solid Te spectrum[53] from which an $N_{\text{eff}}$ value of about 9 is obtained in the 50–150-eV photon-energy range. Its maximum (22 Mb) is about 20% lower than in Xe (28 Mb),[48] whereas the second maximum near 300 eV is 25% higher.[54]

Even if, as Comes, Nielsen, and Schwarz[25] have pointed out, the absorption cross section for $I_2$, on which is based the normalization procedure of the present work, might be 50% higher due to some uncertainties in their experimental procedure, and including our error bars, the maximum intensity value for the total photoabsorption cross section of atomic iodine could not exceed 15 Mb, in good agreement with the value of 17 Mb measured by O'Sullivan in $CH_3I$.[23] It seems that iodine compounds as well as atomic iodine do not follow the general trend. It would be very interesting to continue the experiment beyond 130 eV, in order to see whether or not we find the missing oscillator strength after the $4d$ Cooper minimum. This oscillator strength transfer could be due, in a one-electron central-field model, to a lower overlap between the $4d$ and $\epsilon f$ orbitals at low energy, since the centrifugal barrier in atomic iodine is higher than in xenon.

## IV. CONCLUDING REMARKS

In this first complete $4d$ photoionization study of atomic iodine, we have pointed out some specific open-shell effects such as the strong $4d$-$5d$ hole coupling, as revealed by the $4d$ PES, and the weaker enhancement of the outer-shell cross sections, especially the $5p$ one, in the region of the $4d$ shape resonance, as compared with xenon. Moreover, as in xenon, we stress the importance of multiple-electron excitations for a good understanding of the $4d$ photoionization process. Nevertheless, the question of the absolute photoabsorption maximum intensity, already raised by Comes, Nielsen, and Schwarz[25] in $I_2$ and O'Sullivan in $CH_3I$,[23] is still open in view of our measurements. Now, that theory and experiment are in very good agreement for xenon, we hope that theoreticians will bring some new insights into the photoionization process of open-shell species, such as atomic iodine, which could become a new showcase for atomic inner-shell photoionization.

## ACKNOWLEDGMENTS

It is a pleasure to warmly thank Irène Nenner for her constant scientific support, as well as Marie-Yvonne Adam, Françoise Combet-Farnoux, Göran Wendin, and John W. Cooper for helpful discussions. We are indebted, for general facilities, to the technical staff of the Laboratoire pour l'Utilisation du Rayonnement Electromagnétique, laboratoire mixte du Centre National de la Recherche Scientifique, du Commissariat à l'Energie Atomique et du Ministère de l'Education Nationale. This work has been supported by Contract No. SA 8176/BJ CEA-XRS.

*Also at X-Recherche Service, Parc-Club, 28 rue Jean Rostand, 91893 Orsay CEDEX, France.

†Also at Commissariat à l'Energie Atomique, Département de Physique Générale, Centre d'Etude Nucléaire de Saclay, 91191 Gif-sur-Yvette CEDEX, France.

[1]M. O. Krause, in *Photoionization and Other Probes of Many-Electron Interactions,* edited by F. Wuilleumier (Plenum, New York, 1976), p. 133.

[2]M. Y. Adam, F. Wuilleumier, N. Sandner, S. Krummacher, V. Schmidt, and W. Mehlhorn, Jpn. J. Appl. Phys. **17**, 170 (1978).

[3]S. Southworth, U. Becker, C. M. Truesdale, P. H. Kobrin, D. W. Lindle, S. Owaki, and D. A. Shirley, Phys. Rev. A **28**, 261 (1983).

[4]A. Fahlman, M. O. Krause, T. A. Carlson, and A. Svensson, Phys. Rev. A **30**, 812 (1984).
[5]B. Kammerling, H. Kossman, and V. Schmidt, J. Phys. B **22**, 841 (1989).
[6]U. Becker, D. Szostak, H. G. Kerkhoff, M. Kupsch, B. Langer, R. Wehlitz, A. Yagishita, and T. Hayaishi, Phys. Rev. A **39**, 3902 (1989).
[7]G. Wendin, J. Phys. B **6**, 42 (1973).
[8]M. Ben Amar and F. Combet-Farnoux, J. Phys. B **16**, 2339 (1983).
[9]Z. Altun, M. Kutzner, and H. P. Kelly, Phys. Rev. A **37**, 4671 (1988).
[10]M. Ya Amusia, L. V. Chernysheva, G. F. Gribakin, and K. L. Tsemekhman, J. Phys. B **23**, 393 (1990).
[11]D. L. Ederer, Phys. Rev. Lett. **13**, 760 (1964).
[12]For details see *Giant Resonances in Atoms, Molecules, and Solids,* edited by J. P. Connerade, J. M. Esteva, and R. C. Karnatak (Plenum, New York, 1987).
[13]J. A. R. Samson, Y. Shefer, and G. C. Angel, Phys. Rev. Lett. **56**, 2020 (1986).
[14]M. Pettini, M. Mazzoni, and G. P. Tozzi, Phys. Lett. **82**, 168 (1981).
[15]J. Berkowitz and G. L. Goodman, J. Chem. Phys. **71**, 1754 (1979).
[16]K. Kimura, T. Yamazaki, and Y. Achiba, Chem. Phys. Lett. **58**, 104 (1978).
[17]C. A. De Lange, P. Van der Meulen, and M. J. Van der Meer, J. Mol. Struct. **173**, 215 (1988).
[18]J. Tremblay, M. Larzillière, F. Combet-Farnoux, and P. Morin, Phys. Rev. A **38**, 3804 (1988).
[19]L. Nahon, L. Duffy, P. Morin, F. Combet-Farnoux, J. Tremblay, and M. Larzillière, Phys. Rev. A **41**, 4879 (1990).
[20]S. T. Manson, A. Msezane, A. F. Starace, and S. Shahabi, Phys. Rev. A **20**, 1005 (1979).
[21]F. Combet-Farnoux and M. Ben Amar, J. Electron Spectrosc. Relat. Phenom. **41**, 67 (1986).
[22]A. P. Hitchcock and C. E. Brion, J. Electron Spectrosc. Relat. Phenom. **13**, 193 (1978) (electron-impact measurements).
[23]G. O'Sullivan, J. Phys. B **15**, L327 (1982).
[24]D. W. Lindle, P. H. Kobrin, C M. Truesdale, T. A. Ferret, P. A. Heinmann, H. G. Kerkhoff, U. Becker, and D. A. Shirley, Phys. Rev. A **30**, 239 (1984).
[25]F. J. Comes, U. Nielsen, and W. H. E. Schwarz, J. Chem. Phys. **58**, 2230 (1973).
[26]P. Morin and I. Nenner, Phys. Scr. T **17**, 171 (1987).
[27]I. Nenner, P. Morin, P. Lablanquie, M. Simon, N. Levasseur, and P. Millié, J. Electron Spectrosc. Relat. Phenom. **52**, 623 (1990).
[28]M. Ya Amusia, G. F. Gribakin, V. K. Ivanov, and L. V. Chernysheva, J. Phys. B **23**, 385 (1990).
[29]L. Nahon, J. Tremblay, M. Larzillière, L. Duffy, and P. Morin, Nucl. Instrum. Methods B **47**, 72 (1990).
[30]L. Brewer and J. Tellinghuisen, J. Chem. Phys. **56**, 3929 (1972).
[31]C. N. Yang, Phys. Rev. **74**, 764 (1948).
[32]S. Aksela, H. Aksela, and T. D. Thomas, Phys. Rev. A **19**, 721 (1979).
[33]M. Ben Amar, Thèse d'etat, Orsay, 1984.
[34]K. Codling and R. P. Madden, Phys. Rev. Lett. **12**, 106 (1964).
[35]J. W. Cooper, Phys. Rev. Lett. **13**, 762 (1964).
[36]F. Combet-Farnoux, in *International Conference on Inner-Shell Ionization Phenomena, Atlanta, GA, 1972,* (U.S. Atomic Energy Commission, Oak Ridge, TN, 1972), Vol. 2, p. 1130.
[37]M. Kutzner, V. Radojevic, and H. P. Kelly, Phys. Rev. A **40**, 5052 (1989).
[38]V. Radojevic, M. Kutzner, and H. P. Kelly, Phys. Rev. A **40**, 727 (1989), M. Kutzner, Z. Altun, and H. P. Kelly, *ibid.* **41**, 3612 (1990).
[39]S. P. Shannon, K. Coodling, and J. B. West, J. Phys. B **10**, 825 (1977).
[40]M. Y. Adam, Thèse d'etat, Orsay, 1978.
[41]This Cooper minimum is not the "direct" 5*s* Cooper minimum, but is due to the intershell coupling with the 5*p* subshell. See Ref. 21.
[42]For a complete study see M. Richter, M. Meyer, M. Palher, T. Prescher, E. V. Raven, B. Sonntag, and H. E. Wetzel, Phys. Rev. A **39**, 5666 (1989) and **40**, 7007 (1989).
[43]U. Becker, T. Prescher, E. Schmidt, B. Sonntag, and H. E. Wetzel, Phys. Rev. A **33**, 3891 (1986).
[44]F. Combet-Farnoux (private communication).
[45]T. Hayaishi, A. Yagishita, E. Shigemasa, E. Murakami, and Y. Morioka, Phys. Scr. **41**, 35 (1990).
[46]T. Nagata, M. Yoshino, T. Hayaishi, Y. Itikawa, Y. Itho, T. Koizumi, T. Matsuo, Y. Sato, E. Shigemasa, Y. Takizawa, and A. Yagishita, Phys. Scr. **41**, 47 (1990).
[47]Ch. Dzionk, W. Fiedler, M. V. Lucke, and P. Zimmermann, Phys. Rev. Lett. **62**, 878 (1989).
[48]R. Haensel, G. Keitel, P. Schreiber, and C. Kunz, Phys. Rev. **188**, 1375 (1969).
[49]L. Nahon, P. Morin, F. Combet-Farnoux, and M. Larzillière (unpublished).
[50]F. J. Comes, R. Haensel, U. Nielsen, and W. H. E. Schwarz, J. Chem. Phys. **58**, 516 (1973).
[51]U. Fano and J. W. Cooper, Rev. Mod. Phys. **40**, 441 (1968).
[52]D. J. Kennedy and S. T. Manson, Phys. Rev. A **5**, 227 (1972).
[53]B. Sonntag, T. Tuomi, and G. Zimmerer, Phys. Status Solidi **58**, 101 (1973).
[54]A. P. Lukirskii, I. A. Brytov, and T. M. Zimkina, Opt. Spectrosk. **17**, 438 (1964) [Opt. Spectrosc. **17**, 234 (1964)]; A. P. Lukirskii, I. A. Brytov, and S. A. Gribovskij, *ibid.* **20**, 368 (1966) [**20**, 203 (1966)].